



Numerical Optimization of Carbon Content Equivalent in Heat Affected Zone of Mild Steel Welds

Apaemi, S¹; Achebo, J.P²; Ozigagun, A³

^{1,2,3}. Department of Production Engineering, Faculty of Engineering, University of Benin, P.M.B 1154, Benin City, Edo State, Nigeria

Corresponding authors: apaemistandfast@gmail.com, josephachebo@yahoo.co.uk, rewzigs@yahoo.com

Article Info

Keywords:

numerical, heat affected zone, optimization, carbon content, welding, mild steel, tungsten inert gas

Received 14 January 2021

Revised 25 January 2021

Accepted 15 February 2021

Available online 01 March 2021



<https://doi.org/10.37933/nipes/3.1.2021.12>

<https://nipesjournals.org.ng>

© 2021 NIPES Pub. All rights reserved.

Abstract

The minimization of carbon content percentage in low carbon steel welding was investigated in this study, the optimized welding experiment was done and the carbon content observed was measured and recorded alongside the values of the process parameters. The optimal model was developed based on certain statistical tests, such as goodness of fit, analysis of variance, cooks distance and plot of residual. The ANOVA result showed that the model is very significant; because it has a p- value that is less than 0.005 and the model was observed to be very fit with R-square values of about 95 %. In this study a numerical optimal model to control carbon content percentage in tungsten inert gas welding of low carbon steel has been achieved. This study reveals that current has strong influence on the carbon content percentage. The model's adequacy was tested and showed satisfactory results, however enabling the model to explain the interaction between the process factors and responses and also to minimize the carbon content.

1. Introduction

Low-carbon steels are refined and strengthened by reducing the carbon content in them, this type of steels can be used in place of high strength constructional steels, the reduction of the carbon content improves the weldability and decrease the susceptibility to hydrogen embrittlement. Welding process introduces local hardening in the heat affected zone (HAZ) of the parent plate due to formation of martensite and or bainite. During the welding process temperatures between the solidus temperature (about 1500°C) and (about 875°C) the austenite grain size decreases as the peak temperature falls, with an accompanying decline in hardenability. The hardness gradient across the parent metal HAZ typically shows a maximum hardness immediately adjacent to the fusion boundary with a progressive decrease across the grain coarsened heat affected zone [1]. Thermal cycle and the heat input during welding can affect the strength and toughness of high strength low alloyed steels (HSLA) as this can cause poor toughness in the heat affected zone (HAZ). Research studies revealed that toughness in the grain coarsened heat affected zone (GC HAZ) is low in mild steel welds [2].

The welding process experiences very high temperatures which can cause austenite grain coarsening and the combination of a coarse austenite grain size and rapid cooling results in brittleness. Recent studies discovered that subsequent welding passes tend to damage the microstructure of the material, especially the region closest to the fusion zone known as the intercritically reheated coarse grained HAZ (IC GC HAZ). During the intercritical thermal cycle, some part of the microstructure transforms into austenite structures, the presence of carbon and manganese stabilizes the strength of

the material. On cooling, these high carbon regions transform to pearlite/bainite or martensite-austenite (M-A) constituents[3]. During welding, the percentage content of carbon and niobium affects heat affected zone toughness of HSLA steels, but is related to the distribution and morphology of the M-A constituent, and the matrix microstructure, although its effect is strongly dependent on heat input [4]. A small count of niobium (0.02%) is known to overturn ferrite nucleation at prior austenite grain boundaries and grow the volume fraction of martensite or bainite. The grain refinement and the resultant improvement of base metal mechanical properties, appear to be outweighed by the detrimental effects of martensite formation, when the steel plates are welded. However, other research showed that the addition of low level of vanadium (about 0.05% V) to the low carbon steels reduced the size and area fraction of M-A phase and improved IC GC HAZ toughness [5]. Heat affected zone (HAZ) - formed during welding is an area in which some structural changes in the welded material take place as the result of experienced temperature. The knowledge of a whole area and of subareas of the HAZ is important from practical point of view, since, fine-grained HAZ is in a critical place in terms of creep strength and thermal fatigue. This applies in particular to those technological operations, in which welding technologies are used for manufacturing or repair. The HAZ adjacent to the native material intact by heat has a lower creep resistance than the native material and only at maximum load (immediate tensile strength) appears trans – crystalline breakthrough in the native material [6]. The cracking of the material beyond the HAZ indicates good ultimate strength of joint, but does not guarantee a good creep strength. In the case of creep, the most dangerous place in the welded joint is (as mentioned earlier) the area of fine-grained structure lying in the heat affected zone. The structure of HAZ created as a result of welding affects tendency of joint to the formation of cold cracks, performance properties of welded construction and in particular its resistance to brittle cracking. In addition, in materials that previously worked in conditions of high temperature creep, the HAZ decides on mechanical properties around the weld joint [7].

these values are gradually increased based on modern methods of calculations of service life under conditions of mechanical stress and thermo-mechanical properties [8]. Comparing the size of HAZ for a weld bead on plate and weld bead on joint for mild steel considering the same process parameters, it was observed that the size of the former was larger than the later. The RSM tool was used to model the relationship between the process parameters and the HAZ size and discovered that the behavior was similar for the types of weld bead being studied [9]. An investigation of the effects of SAW process parameters on HAZ properties pointed out that the heat input and wire-feed rate has a positive effect, but welding speed has a negative effect on all HAZ characteristics[10].The heat affected zone observed in submerged arc welding process tends to imparts some weakness on the weld quality the probability of the structural failure increases with a greater size of HAZ a digital image analysis was done on the HAZ area and discovered the grain size were predominantly small [11].

2. Methodology

The optimum percentage of carbon content in a tungsten inert gas low carbon steel weld was investigated in this research study using the response surface methodology. The welding process employs the use of a non -consumable tungsten electrode. Argon gas was used as shielding gas to protect the weld pool from atmospheric interaction. The design expert version 7 was used for the data analysis, the percentage composition of carbon in the base metal was measured using the optical emission spectrometer, while the carbon content equivalent was computed with the equation presented in Equation 1, TIG welding equipment was used to weld the mild steel plates, the equipment used are shown in Figures 1, 2 and 3.

$$CE= C+(Mn+Si)/6+(Cr+Mo+v)/5+(Ni+Cu)/15 \quad (1)$$



Figure 1:TIG welding equipment



Figure 2:Shielding gas regulator



Figure 3: Optical emission spectrometer

2.1 Material selection

Mild steel is mostly preferred by fabrication experts because it is affordable and available. Mild steel material is mostly used for the manufacturing of engineering structures because it possesses good mechanical properties. This grade has high corrosion resistance and can be operated at elevated temperature. The work piece was cut into the following dimensions of specimen: 60mmx40mmx10 mm.

2.2 Welding Process Parameters

The welding process parameters consists of current, voltage, gas flow rate and the range of the process parameters obtained from literature. The Tungsten inert gas welding machine has a regulator, which makes it easy for you to set the current and voltage input values at the desired level, the shielding gas cylinder comes with a regulator with which you can control the gas flow rate, the range of values are shown in Table 1.

Table 1: Process parameters

Parameters	Unit	Symbol	Coded value	Coded value
			Low (-1)	High (+1)
Current	Amp	A	110	150
Gas flow rate	Lit/min	F	25	28
Voltage	Volt	V	11	15

2.3 Conducting the experiments using the design matrix

100 pieces of mild steel coupons measuring 60 x 40 x10 was used for the experiments, the experiment was performed 20 times, using 5 specimens for each run. The weld samples were made from mild steel plate, the plate was cut to size with the power hacksaw. The edges grinded and surfaces polished with emery paper and the joints welded, the responses were measured and recorded. The welding process uses a shielding gas to protect the weld specimen from atmospheric interaction, 100% pure Argon gas was used in this research study. The experimental results are shown in Table 2.

3.Results and Discussion

Table 2: Experimental data

Run	Current	Voltage	Gas flow	CC
1	150.23	26.50	12.50	1.1
2	125.00	26.50	12.50	5.2
3	125.00	26.50	12.50	5.4
4	125.00	26.50	12.50	5.6
5	140.00	25.00	11.00	5
6	125.00	23.98	12.50	6
7	140.00	25.00	14.00	4.5
8	125.00	26.50	15.02	6.7
9	140.00	28.00	11.00	4.2
10	110.00	25.00	14.00	4.9
11	125.00	29.02	12.50	5.7
12	125.00	26.50	12.50	5.7
13	125.00	26.50	9.98	6.2
14	110.00	25.00	11.00	4.8
15	99.77	26.50	12.50	4.3
16	125.00	26.50	12.50	4.8
17	140.00	28.00	14.00	3.25
18	125.00	26.50	12.50	5
19	110.00	28.00	11.00	6.23
20	110.00	28.00	14.00	6.35

To develop an optimal model, certain statistical tests needs to be satisfied of which the goodness of fit is one of them, this diagnostics helps to measure the strength of the model, the goodness of fit table for the carbon content percentage model has a high R square value, indicating that the quadratic model is suitable for the carbon content response, the GOF table is shown in Table 3.

Table 3: Goodness of fit statistics for carbon content equivalent

Std. Dev.	0.37	R-Squared	0.9548
Mean	5.05	Adj R-Squared	0.9141
C.V. %	7.29	Pred R-Squared	0.7805
PRESS	6.56	Adeq Precision	19.810

To further check for the selected models significance, the ANOVA table is needed and a look at the p value can help us check for significance a p value < 0.005 is desired, the ANOVA table is shown in Table 4.

Table 4: ANOVA for carbon content equivalent

	Sum of		Mean	F	p-value	
Source	Squares	Df	Square	Value	Prob > F	
Model	28.55	9	3.17	23.47	< 0.0001	Significant

A-current	8.40	1	8.40	62.16	< 0.0001	
B-voltage	7.756E-003	1	7.756E-003	0.057	0.8155	
C-gas flow rate	0.011	1	0.011	0.082	0.7804	
AB	3.04	1	3.04	22.48	0.0008	
AC	0.35	1	0.35	2.58	0.1394	
BC	0.023	1	0.023	0.17	0.6880	
A^2	12.47	1	12.47	92.22	< 0.0001	
B^2	0.49	1	0.49	3.60	0.0871	
C^2	2.26	1	2.26	16.70	0.0022	
Residual	1.35	10	0.14			
Lack of Fit	0.74	5	0.15	1.22	0.4156	not significant
Pure Error	0.61	5	0.12			
Cor Total	29.90	19				

Some more diagnostics are employed to check for outliers existing in the data, the cooks distance is vital test required to check for data error, the diagnostics case statistics report for the carbon content is shown in Table 5.

Table 5: Diagnostics case statistics report of observed versus predicted carbon content

Stand ard	Actual	Predicted			Internally Studentized	Externally Studentized	Influence on Fitted Value	Cook's	Run
Order	Value	Value	Residual	Leverage	Residual	Residual	DFFITs	Distance	Order
1	4.80	4.85	-0.046	0.670	-0.216	-0.205	-0.292	0.009	14
2	5.00	4.93	0.073	0.670	0.346	0.330	0.470	0.024	5
3	6.23	6.23	-3.235E-003	0.670	-0.015	-0.015	-0.021	0.000	19
4	4.20	3.85	0.35	0.670	1.659	1.848	* 2.63	0.558	9
5	4.90	5.31	-0.41	0.670	-1.958	-2.365	* -3.37	0.777	10
6	4.50	4.56	-0.060	0.670	-0.283	-0.270	-0.385	0.016	7
7	6.35	6.49	-0.14	0.670	-0.645	-0.625	-0.890	0.084	20
8	3.25	3.27	-0.018	0.670	-0.083	-0.079	-0.112	0.001	17
9	4.30	3.97	0.33	0.607	1.413	1.498	1.863	0.309	15
10	1.10	1.34	-0.24	0.607	-1.025	-1.028	-1.279	0.163	1
11	6.00	5.77	0.23	0.607	1.019	1.021	1.270	0.161	6
12	5.70	5.85	-0.15	0.607	-0.631	-0.611	-0.760	0.062	11
13	6.20	6.45	-0.25	0.607	-1.099	-1.112	-1.383	0.187	13
14	6.70	6.36	0.34	0.607	1.487	1.598	1.988	0.342	8
15	5.20	5.29	-0.086	0.166	-0.256	-0.244	-0.109	0.001	2
16	5.00	5.29	-0.29	0.166	-0.852	-0.839	-0.375	0.014	18
17	5.60	5.29	0.31	0.166	0.936	0.929	0.415	0.017	4
18	5.70	5.29	0.41	0.166	1.234	1.271	0.568	0.030	12
19	4.80	5.29	-0.49	0.166	-1.447	-1.544	-0.690	0.042	16
20	5.40	5.29	0.11	0.166	0.340	0.324	0.145	0.002	3

To diagnose the statistical properties of the response surface model, the normal probability plot of carbon content is presented in Figure 4.

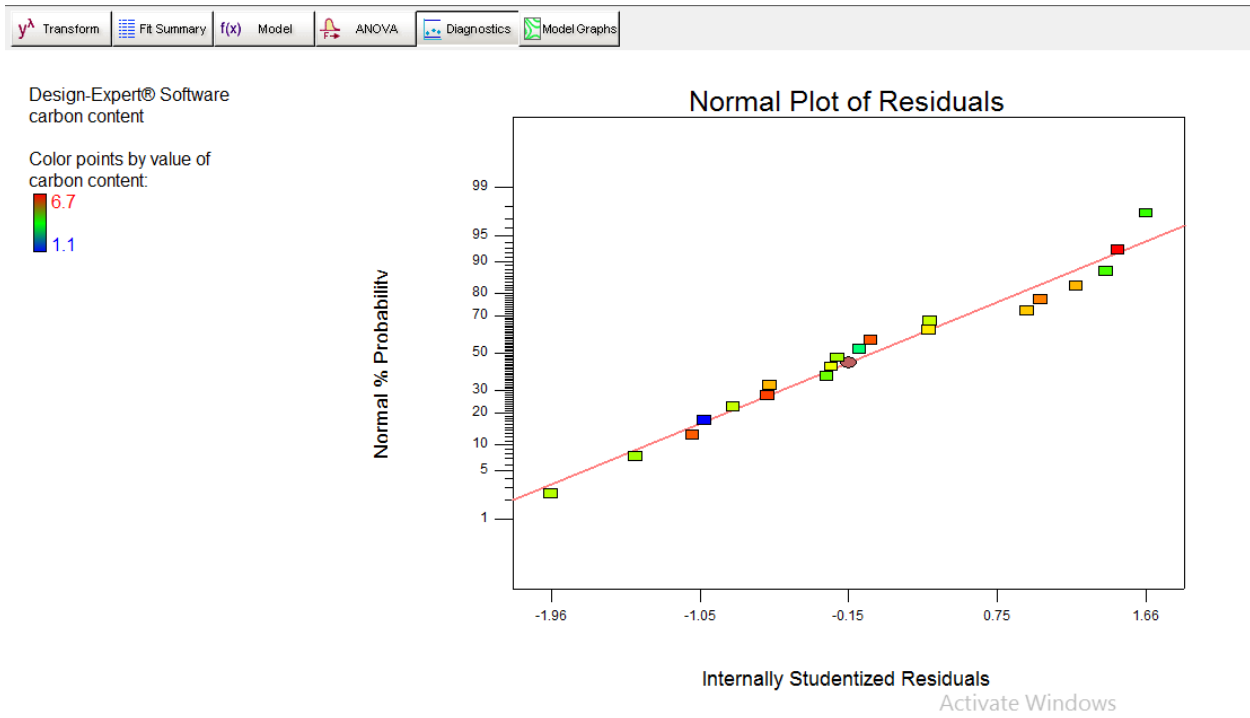


Figure 4: Normal probability plot of studentized residuals for minimizing carbon content

In order to detect a value or group of values that are not easily detected by the model, the predicted values is plotted against the actual values, for carbon content which is shown in Figure 5.

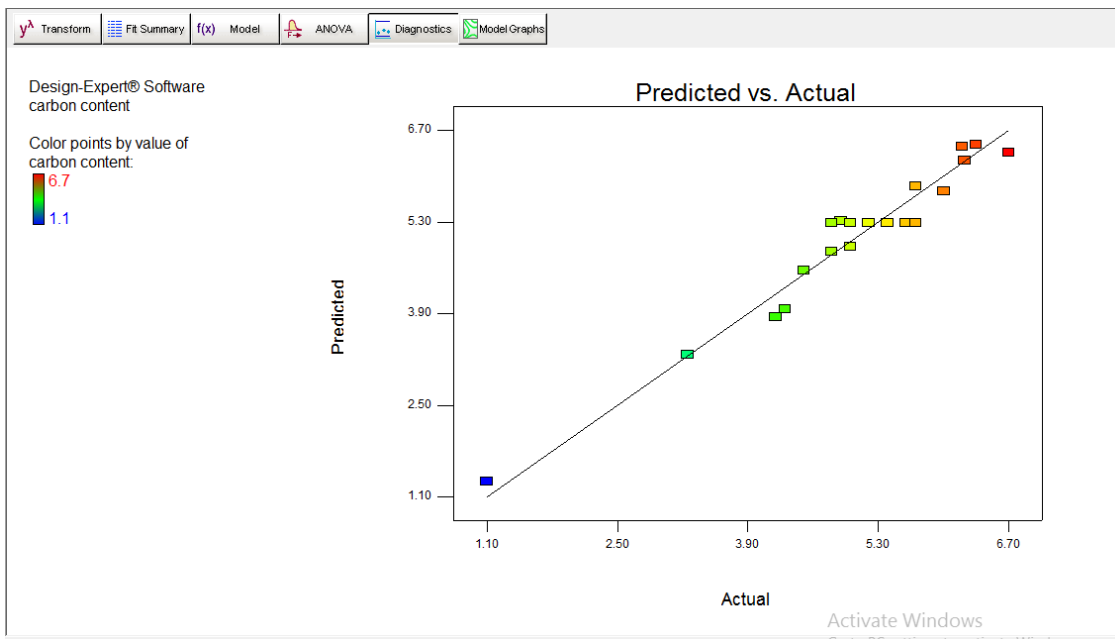


Figure 5: Predicted value Vs actual value for carbon content

To determine the presence of a possible outlier in the experimental data, the cook's distance plot was generated for the carbon content responses. The cook's distance is a measure of how much the regression would change if the outlier is omitted from the analysis. A point that has a very high

distance value relative to the other points may be an outlier and should be investigated. The generated cook's distance for the carbon content is presented in Figures 6.

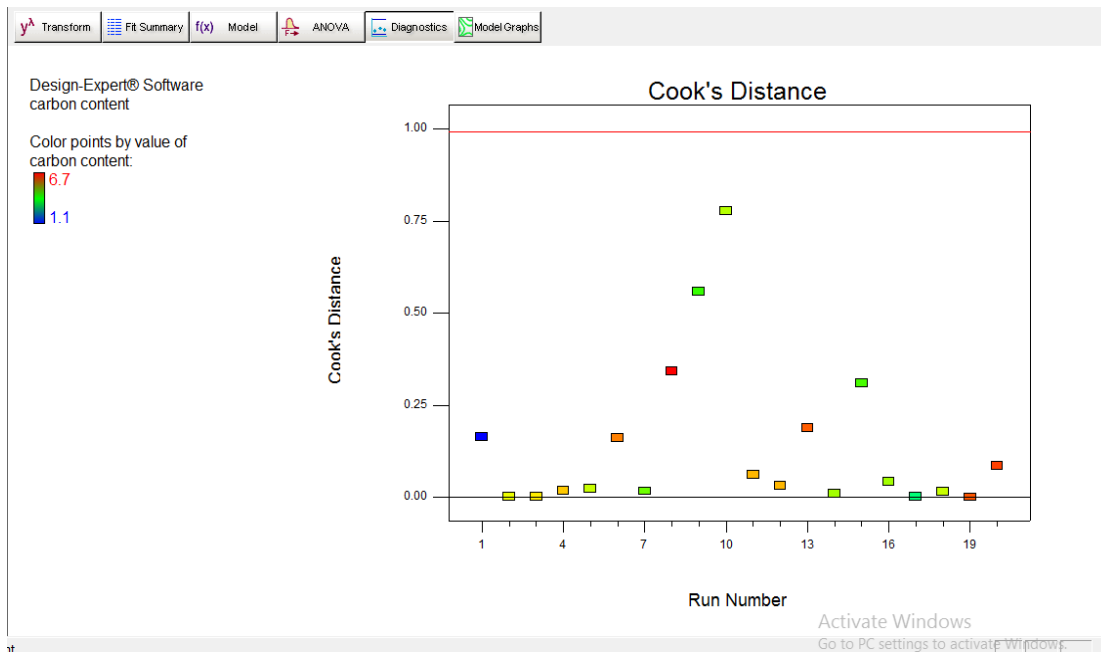


Figure 6: Generated cook's distance for carbon content

The numerical optimal solution was determined for the residual stress and the molten metal viscosity which is shown in Table 6.

Table 6: The numerical optimal solution

Number	CURRENT	VOLTAGE	GAS FLOW RATE	Carbon content	Desirability
1	140.00	28.00	11.00	3.84955	0.908
2	140.00	27.99	11.00	3.8508	0.807
3	140.00	28.00	11.02	3.83651	0.607
4	139.83	28.00	11.00	3.88348	0.605
5	140.00	27.96	11.00	3.85412	0.605
6	139.69	28.00	11.00	3.91195	0.603
7	139.38	28.00	11.00	3.97431	0.597
8	140.00	27.87	11.00	3.86612	0.597
9	140.00	28.00	11.22	3.70094	0.591
10	138.49	28.00	11.00	4.14768	0.581
11	140.00	27.50	11.00	3.92656	0.567
12	140.00	25.23	14.00	4.40682	0.559
13	140.00	25.24	14.00	4.39975	0.559
14	140.00	25.35	14.00	4.33181	0.559
15	139.95	25.21	14.00	4.42895	0.558
16	139.96	25.12	14.00	4.48805	0.558
17	140.00	25.46	14.00	4.26847	0.558
18	139.90	25.40	14.00	4.32078	0.557
19	140.00	28.00	11.66	3.45018	0.553
20	140.00	25.46	13.93	4.24075	0.553
21	139.90	26.28	14.00	3.84668	0.532
22	140.00	26.48	14.00	3.74006	0.524
23	139.43	27.30	14.00	3.55575	0.468
24	140.00	25.79	12.79	3.86702	0.468
25	110.00	25.00	14.00	5.31355	0.442

Table 6 shows the numerical optimal solutions that can minimize the carbon content within this range of process parameters, the results shows that current of 140.00,voltage of 28,00gas flow rate 11 will produce carbon content of 3.84955 .The surface plots showing carbon content variable against the optimized value of current and gas flow rate is presented in Figure 7.

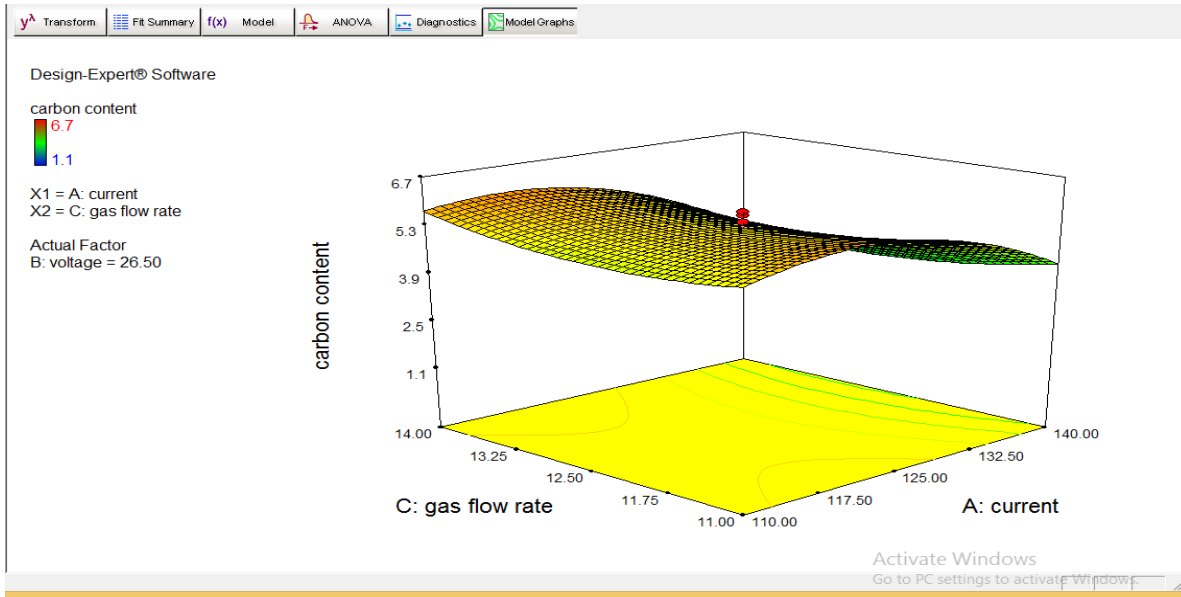


Figure 7: Effect of current and gas flow rate on carbon content

The contour plots showing carbon content response variable against the optimized value of current and voltage is presented in Figure 8.

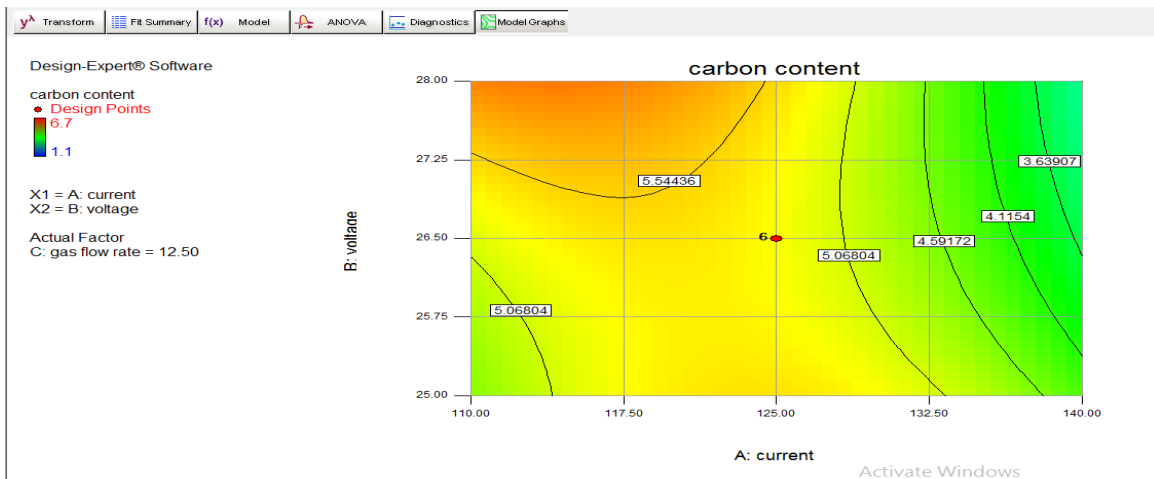


Figure 8: Predicting carbon content using contour plot

3.2 Discussion

The minimization of carbon content percentage in low carbon steel welding was investigated in this study, the optimized welding experiment was done and the carbon content observed was measured and recorded alongside the values of the process parameters. The optimal model was developed based on certain statistical tests, such as goodness of fit, analysis of variance, cooks distance and plot of residual. The ANOVA result showed that the model is very significant; because it has a p-value that is less than 0.005. The numerical optimal solutions that can minimize the carbon content within this range of process parameters has the following results, current of 140.00,voltage of 28,00

and gas flow rate 11 will produce carbon content of 3.84955. The average carbon content equivalent value observed in the experiment was about 4.3, now the model has successfully minimized the carbon content equivalent by about 21%, with a model adequacy with R-square value of about 95% which is in reasonable agreement with the work of [12] that a coefficient of determination greater than 80% indicates high strength.

4. Conclusion

In this study a numerical optimal model to control carbon content percentage in tungsten inert gas welding of low carbon steel has been achieved. This study reveals that current has strong influence on the carbon content percentage. The model's adequacy was tested by the ANOVA, GOF and cooks distance which showed satisfactory results, which indicates the strength of the model.

References

- [1] R. W. K. Honeycombe and H.K.D.H. Bhadeshia: "Steels – Microstructure and Properties", 2nd Edition, Edward Arnold, 1995.
- [2] K. Easterling: Introduction to the Physical Metallurgy of Welding, Butterworth-Heinemann, Oxford, (1992).
- [3] S. Okaguchi, T. Hashimoto and H. Ohtani: Int. Conf. on Physical Metallurgy of Thermomechanical Processing of Steels and Other Metals, ed. by I. Tamura, ISIJ, Tokyo, (1988), 330.
- [4] J.R. Davis, and King., *Surface Hardening of Steels: Understanding the basics*. Material Park, OH: ASM International, 2002, pp. 242-263.
- [5] H. K. Lee, H. S. Han, K. J. Son and S. B. Hong, Optimization of Nd-Yag Laser Welding Parameters For Sealing Small Titanium Tube Ends, *J. Of Materials Science and Engineering*, Vol. A415, 2006, Pp. 149-155.
- [6] E.S. Dzikowski, J. Banach, (1998). "Working conditions and the potential damage of energy pipelines with respect to welding technology" [in Polish], Proceedings of 1-st scientific-technical conference Pire-98, isbn 83-909539-5-1, 57-62,
- [7] T. Jóźwik, (1998). Steels cr-mo-v for work at elevated temperatures after long-term operation problems of welding" [in Polish], Proceedings of 1-st scientific-technical conference Pire-98, isbn 83-909539-5-1, 69-80
- [8] A.Rusin, A. Wojaczek, M. Bieniek(2012).", selected problems of sustainability assessment and decision support of repair of components of power units with long service life "[in Polish], 11, 738-742
- [9] V. Gunaraj And N. Murugan, Prediction and Comparison of the Area of the Heat-Affected Zone for the Bead-Onplates And Bead-On-Joint In Submerged Arc Welding Of Pipes, *J. Of Materials Processing Tech.*, Vol. 95, 1999, Pp. 246-261.
- [10] V. Gunaraj And N. Murugan, Prediction and Optimization Of Weld Bead Volume For The Submerged Arc Processpart 2, *Welding Journal*, Aws, November 2000, 331-S – 338-S.
- [11] Ghosh A, Chattopadhyaya S, Das R K and Sarkar P K 2011a Assessment of heat affected zone of submerged arc welding process through digital image processing. *Procedia Engineering* 10: 2782–2785
- [12] N.A.Imhansoloeva, J.I Achebo, K.Obahiagbon, J.O. Osarenmwinda and C.E Etinosa (2018) "Optimization of the deposition rate of tungsten inert gas mild steel using the response surface methodology(2018)scientificresearchpublishing Vol.10, 2018 pp 784-804